Relationship Between Neutrophil-Binding Affinity and Suitability for Infection Imaging: Comparison of ^{99m}Tc-Labeled NAP-2 (CXCL-7) and 3 C-Terminally Truncated Isoforms

Huub J.J.M. Rennen, MSc[1]; Cathelijne Frielink[1]; Ernst Brandt, PhD[2]; Sebastian A.J. Zaat, PhD[3]; Otto C. Boerman, PhD[1]; Wim J.G. Oyen, MD[1]; and Frans H.M. Corstens, MD[1]

[1]Department of Nuclear Medicine, University Medical Center Nijmegen, Nijmegen, The Netherlands; [2]Department of Immunology and Cell Biology, Forschungszentrum Borstel, Borstel, Germany; and [3]Department of Medical Microbiology, Academic Medical Center, Amsterdam, The Netherlands

The CXC chemokines are a family of closely related chemoattractant cytokines that bind to, attract, and activate neutrophils to variable degrees. In this study, the relationship between neutrophil-binding affinity and suitability for infection imaging was investigated in a selected group of CXC chemokines. Neutrophil–activating peptide-2 (NAP-2, 70 residues; also called CXCL7) binds with high affinity to the CXCR2 receptor on neutrophils. Recently, C-terminally truncated NAP-2-variants have been described that have enhanced neutrophil-binding affinity and neutrophil-stimulating capacity. Here, NAP-2 and its C-terminal shortened variants NAP-2(1–68), NAP-2(1–66), and NAP-2(1–63) were labeled with ^{99m}Tc via the hydrazinonicotinamide (HYNIC) chelator and their potential for imaging of infection was investigated in a rabbit model of infection. The CXC chemokine interleukin-8 (IL-8) was used for comparison. In addition, a series of ^{99m}Tc-labeled CXC chemokines were screened for their potential to image infection, including CTAP-III, GCP-2, ENA-78, PF-4, and IP-10. **Methods:** The receptor-binding affinity of HYNIC-conjugated NAP-2 and its analogs was compared in competitive binding assays on Jurkat cells transfected with the CXCR2 receptor gene. Biodistribution of labeled NAP-2 (analogs) and other CXC chemokines in rabbits with intramuscular *Escherichia coli* infections was determined both by γ-camera imaging and by counting dissected tissues at 6 h after injection. **Results:** The CXCR2-binding affinity of the HYNIC-conjugated NAP-2 analogs relative to NAP-2 was as follows: NAP-2(1–68), 2.5-fold; NAP-2(1–66), 10-fold; and NAP-2(1–63), 3-fold. In the rabbit model, uptake in the abscess (in percentage injected dose per gram ± SEM) was 0.084 ± 0.015 for NAP-2, 0.098 ± 0.010 for NAP-2(1–68), 0.189 ± 0.044 for NAP-2(1–66), and 0.114 ± 0.017 for NAP-2(1–63) at 6 h after injection. In comparison, higher uptake in the abscess was found for labeled IL-8, a modest uptake was found for GCP-2 and ENA-78, and a low uptake was found for CTAP-III, PF-4, and IP-10. **Conclusion:** This study showed a clear relationship between affinity to receptors on neutrophils and suitability for infection imaging. Of the NAP-2 variants, NAP-2(1–66) combined highest affinity to CXCR2 with the best characteristics for imaging. IL-8 binds to both CXCR1 and CXCR2 with high affinity and showed a superior imaging quality. The other CXC chemokines tested bind to neutrophils with lower affinity and were shown to be less suitable for infection imaging in this study.

Key Words: infection imaging; ^{99m}Tc; NAP-2 analogs

J Nucl Med 2004; 45:1217–1223

White blood cells, particularly neutrophils and monocytes, accumulate in high numbers at sites of infection. They function as the primary line of defense in the destruction of microorganisms and initiate the repair of tissue. A variety of chemotactic peptides and proteins orchestrate the directed migration of leukocytes to inflammatory sites. Potentially, these leukocyte-binding proteins can be used as an infection imaging agent, labeled either in their original natural form or in the sophisticated disguise of a receptor antagonist (*1*). This study focuses on a selection of chemokines for infection imaging.

The chemokines (short for chemoattractant cytokines) are a superfamily of closely related cytokines. Most of the chemokines are small, with molecular weights in the range of 8–12 kDa. The chemokine superfamily is divided into subfamilies depending on the position of the highly conserved cysteines (*2*). One major subfamily is designated "CXC" because the 2 cysteines (C) nearest the N-termini of these proteins are separated by a single, nonconserved amino acid residue (X). The other major subfamily is called "CC" because these 2 cysteines are adjacent. The CXC chemokines act predominantly on neutrophils, whereas the CC chemokines act on lymphocytes, monocytes, mast cells, and eosinophils (*3*). The CXC chemokine subfamily can be further divided into ELR^+ and ELR^- CXC chemokines

Received Nov. 6, 2003; revision accepted Jan. 14, 2004.

For correspondence or reprints contact: Huub J.J.M. Rennen, MSc, Department of Nuclear Medicine, University Medical Center Nijmegen, P.O. Box 9101, 6500 HB Nijmegen, The Netherlands.

E-mail: h.rennen@nucmed.umcn.nl

depending on the presence or absence of a Glu-Leu-Arg (ELR) motif, respectively. This motif is positioned in the NH_2-terminal region just in front of the first cysteine of the CXC motif. The ELR^+ CXC chemokines are the most selective chemotactic factors for neutrophil migration. Interleukin-8 (IL-8; recently renamed CXC chemokine ligand 8 [CXCL8] (*4*)) is the prototype of this group and is the most potent neutrophil-activating protein of the CXC chemokines in the human system (*2*,*5*,*6*). Other members of this group include growth-regulated oncogene (GROα [CXCL1], GROβ [CXCL2], and GROγ ([CXCL3]), connective tissue–activating peptide-III (CTAP-III), neutrophil- activating protein-2 (NAP-2 [CXCL7]), epithelial cell–derived neutrophil attractant-78 (ENA-78 [CXCL5]), and granulocyte chemotactic protein-2 (GCP-2 [CXCL6]). The ELR^- CXC chemokines include platelet factor-4 (PF-4 [CXCL4]) and interferon-γ–inducible protein (IP-10 [CXCL10]).

There are 2 high-affinity G protein-coupled CXC chemokine receptors on neutrophils: CXC chemokine receptor 1 (CXCR1) and CXCR2 (*7*). IL-8 and GCP-2 bind to both CXCR1 and CXCR2, whereas the other ELR^+ CXC chemokines are specific ligands for CXCR2 (*8*,*9*). The ELR^- CXC chemokines PF-4 and IP-10 lack significant CXCR1 and CXCR2 binding (*10*,*11*). PF-4 is reported to be active on many different cell types, including neutrophils (*12*), but no G protein–coupled receptor has been identified for PF-4 so far.

In this study, we aimed to select the most promising candidates within the family of the CXC chemokines. Is there a clear relationship between biologic properties such as neutrophil chemoattractant activity (as can be assessed in Boyden chamber assays), neutrophil-activating properties (e.g., elastase release), and neutrophil-binding affinity on the one side and suitability for infection imaging on the other side? We hypothesize that neutrophil-binding affinity is a useful criterion for selecting the most suitable CXC chemokine for infection imaging. This study focuses on NAP-2 and 3 C-terminally truncated NAP-2 variants. NAP-2 is a member of a group of CXC chemokines collectively termed β-thromboglobulins (*12*). These are platelet α-granule–derived proteins, which differ only in the length of the termini. Platelet basic protein ([PBP] 94 residues) and CTAP-III (85 residues) were shown to become converted into NAP-2 (70 residues) by N-terminal truncation through limited proteolysis (*13*,*14*). Although structurally closely related, the β-thromboglobulins PBP and CTAP-III do not exhibit neutrophil-stimulatory activity in contrast to their proteolytic daughter compound NAP-2. Recently, C-terminally truncated NAP-2-variants have been described that have enhanced affinity for receptors on neutrophils and enhanced neutrophil-stimulating capacity (*15*,*16*). NAP-2(1–68) is also named thrombocidin-1 (TC-1) and has bactericidal properties (*17*). Here, NAP-2 and its C-terminally shortened variants NAP-2(1–68), NAP-2(1–66), and NAP-2(1–63) were labeled with ^{99m}Tc and their potential for imaging infection was investigated in rabbits with intramuscular *Escherichia coli* infection. IL-8, binding to both CXCR1 and CXCR2 with high affinity, has already been studied in detail for infection imaging purposes and was used for comparison (*18*–*20*).

In addition, a broad inventory of the CXC chemokines for infection imaging was made. CTAP-III, GCP-2, and ENA-78 (ELR^+ CXC chemokines) and PF-4 and IP-10 (ELR^- CXC chemokines) are a representative selection of the CXC chemokines that were tested in our laboratory using the same rabbit model of intramuscular infection as used above.

MATERIALS AND METHODS

Chemokines

The following human recombinant proteins were used: NAP-2 was purchased from RDI. NAP-2(1–68), NAP-2(1–66), and NAP-2(1–63) were produced by recombinant methods as described previously (*12*). IL-8 was kindly provided by Dr. Ivan Lindley (Novartis). GCP-2, ENA-78, and IP-10 were purchased from RDI. CTAP-III and PF-4 were kindly provided by Dr. Alfred Waltz (Theodor-Kocher Institute, University of Bern, Bern, Switzerland).

Conjugation of Hydrazinonicotinamide (HYNIC) to Chemokine

The propylaldehyde hydrazone of succinimidyl-hydrazinonicotinamide (HYNIC) was synthesized essentially as described previously (*3*,*21*). The HYNIC-chemokine conjugate was prepared as described previously (*18*). Briefly, in a 1.5-mL vial, 5 μL of 1 mol/L $NaHCO_3$, pH 8.2, was added to 35 μL of chemokine (5 mg/mL). Subsequently, a 3-fold molar excess of HYNIC in 5 μL of dry dimethyl sulfoxide was added dropwise to the mixture. After incubation for 10–30 min at room temperature, the reaction was stopped by adding an excess of glycine (200 μL, 1 mol/L in phosphate-buffered saline [PBS]). To remove excess unbound HYNIC, the mixture was extensively dialyzed against PBS (0.1- to 0.5-mL dialysis cell, 3.5-kDa molecular weight cutoff; Pierce). Dialyzed samples of about 8 μg HYNIC-conjugated chemokine were stored at −20°C.

^{99m}Tc Labeling of HYNIC-Conjugated Chemokine

Tricine (*N*-[Tris(hydroxymethyl)methyl]glycine) was purchased from Fluka and nicotinic acid was from Sigma-Aldrich. For labeling of the HYNIC-conjugated chemokines with ^{99m}Tc, tricine and nicotinic acid were used as coligands as described previously (*19*). To a thawed sample of 8 μg of HYNIC-chemokine was added 0.2 mL of a solution of tricine and nicotinic acid (125 and 12.5 mg/mL, respectively, in PBS, adjusted to pH 7.0 with 2 mol/L NaOH), 20 μL of a freshly prepared tin(II) solution (10 mg $SnSO_4$ in 10 mL of nitrogen-purged 0.1N HCl), and 300–400 MBq $^{99m}TcO_4^-$ in saline. The mixture was incubated at 70°C for 30 min.

The radiochemical purity was determined by instant thin-layer chromatography (ITLC) on ITLC-SG strips (Gelman Laboratories) with 0.1 mol/L citrate, pH 6.0, as the mobile phase. In case of a labeling efficiency of <96%, the reaction mixture was applied to a Sephadex G-25 column (PD-10; Pharmacia) and eluted with PBS/0.5% bovine serum albumin (BSA) to purify the radiolabeled chemokine. For animal experiments, the reaction mixture was diluted with PBS/0.5% BSA to a concentration of 40 MBq/mL, ready for intravenous administration in the rabbits.

Receptor-Binding Competition Assays

The interaction of HYNIC-conjugated NAP-2, its variants, and IL-8 with chemokine receptor CXCR2 was investigated in binding competition assays using a single concentration of ^{99m}Tc-labeled IL-8 and increasing concentrations of the unlabeled chemokines. These assays were performed using Jurkat cells transfected with the CXCR2 receptor, a kind gift of Drs. Pius Loetscher and Marco Baggiolini (Theodor Kocher Institute, University of Bern, Bern, Switzerland) (*22*). The Jurkat cells were cultured at 37°C in a humidified atmosphere of 95% air/5% CO_2 in RPMI 1640 medium (GIBCO) containing 10% fetal calf serum and 1% glutamine, amino acids, and pyruvate. The medium also contained penicillin/streptomycin, 5×10^{-5} mol/L β-mercaptoethanol, and 1.5 μg/mL puromycin for selection. Live Jurkat cells were centrifuged (5 min, 2,000*g*) and washed once with assay buffer (RPMI 1640, 0.5% BSA, 0.05% NaN_3). For the receptor-binding competition assays, CXCR2-bearing Jurkat cells were suspended at $\sim 4 \times 10^8$ cells per milliliter (final concentration) in RPMI 1640 medium containing 0.5% BSA. Duplicate samples of $\sim 2 \times 10^8$ cells were incubated on ice for 3 h with a constant amount of ^{99m}Tc-labeled IL-8 ($\sim$0.014 nmol/L IL-8, $\sim$50,000 counts of radioactivity) as a tracer, in the presence or absence of increasing concentrations (0.25–400 nmol/L) of HYNIC-conjugated NAP-2, its variants, and IL-8 in a total volume of 0.5 mL. To correct for nonspecific binding of ^{99m}Tc-labeled IL-8, a sample was incubated in the presence of a 30,000-fold excess of native IL-8. After a 3-h incubation on ice, cells were centrifuged (5 min, 2,000*g*) and washed twice with incubation buffer, and the radioactivity in the pellet (total bound radioactivity) was measured in a shielded well-type γ-counter (Wizard; Pharmacia). Nonspecific binding of ^{99m}Tc-labeled IL-8 was subtracted. Each assay was performed in duplicate. The concentration of HYNIC-conjugated NAP-2 that caused 50% displacement was set at 1 and the 50% inhibitory concentrations of the HYNIC-conjugated NAP-2 variants and IL-8 were expressed relative to that of HYNIC-conjugated NAP-2.

Animal Studies

For a direct comparison between ^{99m}Tc-labeled NAP-2, its 3 C-terminally truncated variants, and IL-8 in imaging intramuscular infection, abscesses were induced in the left thigh muscle of 25 female New Zealand White rabbits (2.4–2.7 kg) with $1–2 \times 10^{11}$ colony-forming units (cfu) of *E. coli* in 0.5 mL. During the procedure, rabbits were anesthetized with a subcutaneous injection of a 0.6-mL mixture of fentanyl (0.315 mg/mL) and fluanisone (10 mg/mL) (Hypnorm; Janssens Pharmaceutical). The rabbits were divided into 5 groups of 5 animals each (5 animals per ^{99m}Tc-labeled chemokine). After 24 h, when swelling of the muscle was apparent, the rabbits were injected with 20 MBq ^{99m}Tc-labeled chemokine (protein dose, 0.5 μg) via the ear vein. Three rabbits from each group were used for γ-camera imaging. These rabbits were immobilized, placed prone on the γ-camera, and images were recorded at 1–5 min and 1½, 3, 4½, and 6 h after injection with a single-head γ-camera (Orbiter; Siemens Medical Systems Inc.) equipped with a parallel-hole, low-energy, all-purpose collimator. Images were obtained with a 15% symmetric window over the 140-keV energy peak of ^{99m}Tc. After acquisition of 200,000–300,000 counts, the images were digitally stored in a 256 × 256 matrix.

Scintigraphic images were analyzed quantitatively by drawing regions of interest over the abscess and the uninfected contralateral thigh muscle (background). Abscess-to-background ratios were calculated.

After completion of the final imaging session (6 h after injection), all rabbits were killed with a lethal dose of pentobarbital (Euthesate; Ceva Sante Animale). Samples of blood, infected thigh muscle, uninfected contralateral thigh muscle, lung, spleen, liver, kidneys, and intestines were collected. The dissected tissues were weighed and counted in a γ-counter. To correct for radioactive decay, injection standards were counted simultaneously. The measured activity in samples was expressed as the percentage of injected dose per gram tissue (%ID/g). Abscess-to-contralateral muscle ratios and abscess-to-blood ratios were calculated.

Using the same rabbit model of intramuscular infection, the ^{99m}Tc-labeled CXC chemokines CTAP-III, GCP-2, ENA-78, PF-4, and IP-10 were tested for infection imaging in pilot experiments using 2 rabbits per ^{99m}Tc-labeled CXC chemokine.

Statistical Analysis

All mean values are given as %ID/g, %ID, or ratios ± 1 SEM. The data were analyzed statistically using the 1-way ANOVA with the Dunnett posttest (GraphPad Instat 3.00 Win 95) comparing data for the ^{99m}Tc-labeled NAP-2 derivatives with data for ^{99m}Tc-labeled NAP-2.

RESULTS

^{99m}Tc Labeling of Chemokines

The radiochemical purities of ^{99m}Tc-labeled NAP-2, its variants, and IL-8 exceeded 98% in all cases, as determined by ITLC, excluding the need for further purification. This is in line with our previous findings for IL-8, where the same labeling strategy using tricine and nicotinic acid as coligands was adopted (*19*). The specific activities of the preparations of ^{99m}Tc-labeled NAP-2, its variants, and IL-8 were high, approximately 40–50 MBq/μg of protein. The specific activities of the preparations of ^{99m}Tc-labeled CTAP-III, GCP-2, ENA-78, PF-4, and IP-10 ranged from 20 to 40 MBq/μg of protein.

Receptor-Binding Competition Assays

The receptor-binding competition assays involved a direct comparison in binding to the CXCR2 receptor between HYNIC-conjugated proteins—that is, chemically modified proteins. The relative potencies of HYNIC-conjugated NAP-2 and its 3 C-terminally truncated variants for binding to CXCR2 receptors transfected on Jurkat cells are depicted in Figure 1. A 2- to 3-fold higher binding potency was found for the HYNIC-conjugated forms of NAP-2(1–68) and NAP-2(1–63) as compared with NAP-2. HYNIC-conjugated NAP-2(1–66) showed a 10-fold higher binding potency relative to NAP-2. For comparison, the binding potency of HYNIC-conjugated IL-8 was 75-fold higher.

Animal Studies

Table 1 summarizes the biodistribution results of the 4 radiolabeled chemokine preparations in rabbits with an *E. coli* infection at 6 h sfter injection. Figure 2 presents uptake of the 4 radiolabeled chemokines in neutrophil-rich tissues—that is, the abscess, the lungs, and the spleen. ^{99m}Tc-

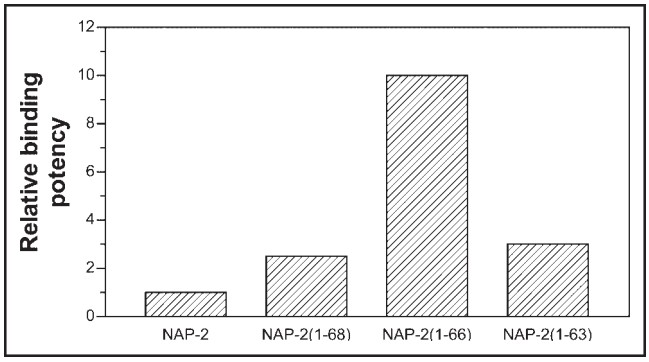

FIGURE 1. Relative potencies of HYNIC-conjugated NAP-2 and 3 C-terminally truncated variants to compete with ^{99m}Tc-labeled IL-8 for binding to Jurkat cells transfected with CXCR2 receptor. Potency of HYNIC-conjugated NAP-2 is set at 1.

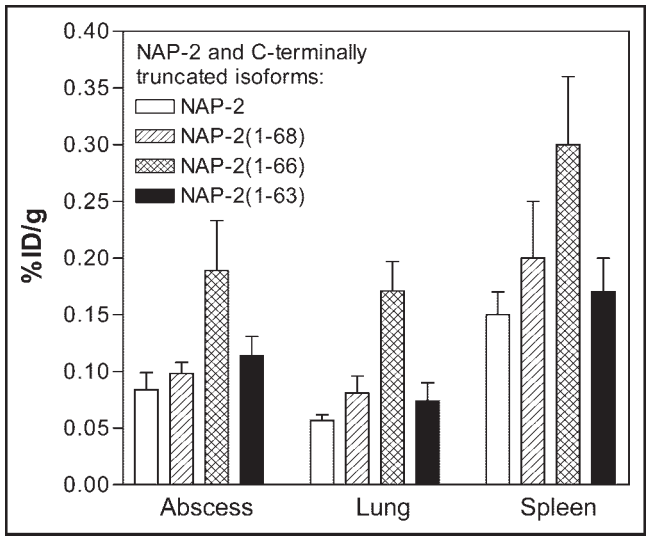

FIGURE 2. Uptake of ^{99m}Tc-labeled NAP-2 and 3 C-terminally truncated variants at 6 h after injection in tissues with high natural abundancy of neutrophils: abscess, lungs, and spleen. Values are expressed as %ID/g ± 1 SEM.

Labeled NAP-2(1–66) showed higher uptake in the abscess ($P < 0.05$) as compared with ^{99m}Tc-labeled NAP-2. Physiologic uptake in the lungs was significantly higher for ^{99m}Tc-labeled NAP-2(1–66) as well ($P < 0.01$). Abscess-to-muscle and abscess-to-blood ratios showed no significant differences. The agents cleared predominantly via the kidneys, and the residual amount of radioactivity in the kidneys was significantly lower ($P < 0.01$) for the 2 shortest labeled NAP-2 variants, NAP-2(1–66) and NAP-2(1–63), as compared with NAP-2. In comparison with ^{99m}Tc-labeled NAP-2, IL-8 showed significantly higher uptake in the abscess (0.39 ± 0.09 %ID/g), the lungs (0.12 ± 0.01 %ID/g), and the spleen (0.55 ± 0.13 %ID/g) and higher abscess-to-muscle ratios (215 ± 90) and abscess-to-blood ratios (24 ± 4).

Figure 3 shows the scintigrams acquired between 0 and 6 h after injection of ^{99m}Tc-labeled NAP-2 and its 3 C-terminally truncated variants. γ-Camera imaging rapidly visualized the abscess from a few hours after injection onward for all preparations. Quantitative analysis of the images revealed that the abscess-to-background ratios improved with time for all labeled chemokines up to 9 ± 1 for NAP-2, 9 ± 2 for NAP-2(1–68), 13 ± 1 for NAP-2(1–66), and 10 ± 1 for NAP-2(1–63) at 6 h after injection. For comparison, ^{99m}Tc-IL-8 generated an abscess-to-background ratio of 20 ± 4 in the same animal model. Immediately after injection, high kidney uptake was observed for all preparations, remaining prominent throughout the study.

An overview of the various radiolabeled CXC chemokines studied in the same rabbit model of intramuscular infection is presented in Figure 4. Figure 4 contains representative images of ^{99m}Tc-labeled IL-8 (high affinity for

TABLE 1
Biodistribution of ^{99m}Tc-Labeled NAP-2 and 3 C-Terminally Truncated Variants in Rabbits with *Escherichia coli*–Induced Intramuscular Infection

Parameter	^{99m}Tc-NAP-2	^{99m}Tc-NAP-2(1–68)	^{99m}Tc-NAP-2(1–66)	^{99m}Tc-NAP-2(1–63)
Biodistribution				
Blood	0.015 ± 0.001	0.013 ± 0.002	0.017 ± 0.003	0.013 ± 0.002
Muscle	0.0017 ± 0.0002	0.0016 ± 0.0002	0.0024 ± 0.0001	0.0018 ± 0.0003
Abscess	0.084 ± 0.015	0.098 ± 0.010	0.189 ± 0.044	0.114 ± 0.017
Lung	0.057 ± 0.005	0.081 ± 0.015	0.171 ± 0.026	0.074 ± 0.016
Spleen	0.15 ± 0.02	0.20 ± 0.05	0.30 ± 0.06	0.17 ± 0.03
Kidney	3.1 ± 0.1	3.0 ± 0.1	1.9 ± 0.1	2.3 ± 0.1
Liver	0.032 ± 0.001	0.035 ± 0.001	0.048 ± 0.006	0.043 ± 0.007
Intestine	0.011 ± 0.001	0.012 ± 0.001	0.016 ± 0.002	0.014 ± 0.001
Ratio				
Abscess/muscle	52 ± 11	65 ± 11	80 ± 23	66 ± 14
Abscess/blood	5.7 ± 1.3	8.0 ± 1.1	12 ± 3	8.8 ± 1.2

Rabbits were injected with 20 MBq ^{99m}Tc-labeled chemokine, killed at 6 h after injection, and dissected. Tissue samples were weighed and counted in a γ-counter. Values are expressed as %ID/g tissue ± 1 SEM or as ratios thereof.

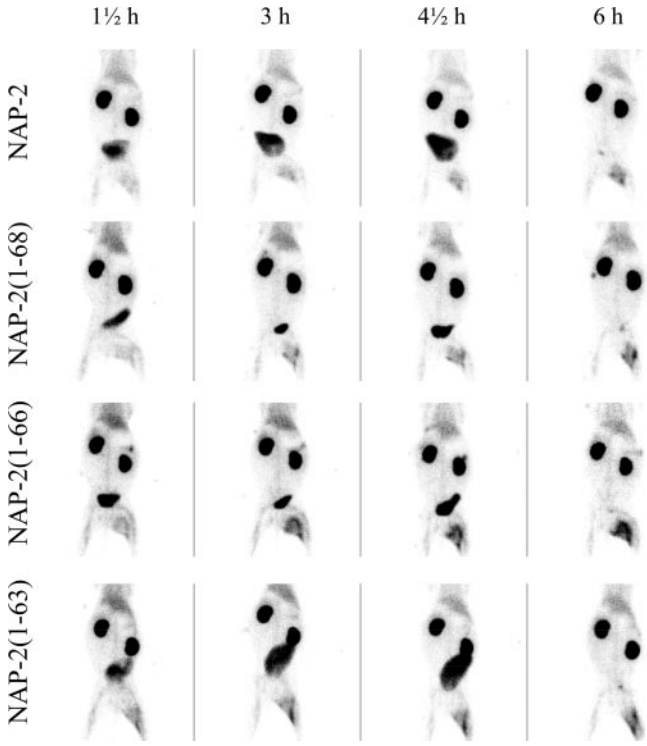

FIGURE 3. Images of rabbits with an *E. coli*–induced abscess in left thigh muscle (right side on image) at 1½, 3, 4½, and 6 h after injection of ^{99m}Tc-labeled NAP-2 and 3 C-terminally truncated variants.

both CXCR1 and CXCR2), CTAP-III (no binding to CXCR2), NAP-2, and its variants (various affinities for CXCR2), GCP-2 (acts via both CXCR1 and CXCR2), and ENA-78 (high affinity for CXCR2). Two examples of ELR$^-$ CXC chemokines with poor neutrophil attractant capacity and no binding to CXCR1 and CXCR2 are PF-4 and IP-10. Figure 4 illustrates the good characteristics for infection imaging of various ^{99m}Tc-labeled ELR$^+$ CXC chemokines, especially for NAP-2(1–66) and IL-8. In comparison with abscess uptake of NAP-2(1–66) (0.189 %ID/g) and IL-8 (0.39 %ID/g), only modest uptake was found for GCP-2 (0.081 %ID/g) and ENA-78 (0.056 %ID/g), and low uptake was found for CTAP-III (0.016 %ID/g), PF-4 (0.016 %ID/g), and IP-10 (0.0052 %ID/g).

DISCUSSION

To select the most suitable candidate for infection imaging within the family of CXC chemokines, we screened a series of ^{99m}Tc-labeled CXC chemokines for infection imaging. In this study, we focused on the relationship between binding affinity toward the CXCR2 receptor and suitability for infection imaging in a selected group of CXC chemokines: NAP-2 (70 residues) and 3 C-terminally truncated variants: NAP-2(1–68), NAP-2(1–66), and NAP-2(1–63). It was previously shown that limited and defined truncation at the C-terminus of native NAP-2 enhances receptor binding and degranulation activity (*15,16*). A most prominent increase in potency to stimulate neutrophil degranulation and to bind neutrophils was observed for isoforms of NAP-2 with a C-terminal deletion of 4 amino acids (NAP-2(1–66)) and 7 amino acids (NAP-2(1–63)). Here, NAP-2 and its 3 variants were conjugated with the bifunctional chelator HYNIC, which links ^{99m}Tc to protein via primary amino groups within the protein. In receptor-binding competition assays, the relative binding affinities of the HYNIC-conjugated (i.e., chemically modified) proteins were determined and the highest binding potency for the CXCR2 receptor was found for NAP-2(1–66). This finding correlated well with the findings of the infection imaging experiments with ^{99m}Tc-labeled NAP-2 and its variants. ^{99m}Tc-Labeled NAP-2(1–66) showed the highest uptake in the abscess and the highest physiologic uptake in the lungs, an organ that accommodates large numbers of neutrophils. HYNIC-conjugated IL-8 had a higher affinity for the CXCR2 receptor and ^{99m}Tc-labeled IL-8 displayed the highest uptake in the abscess.

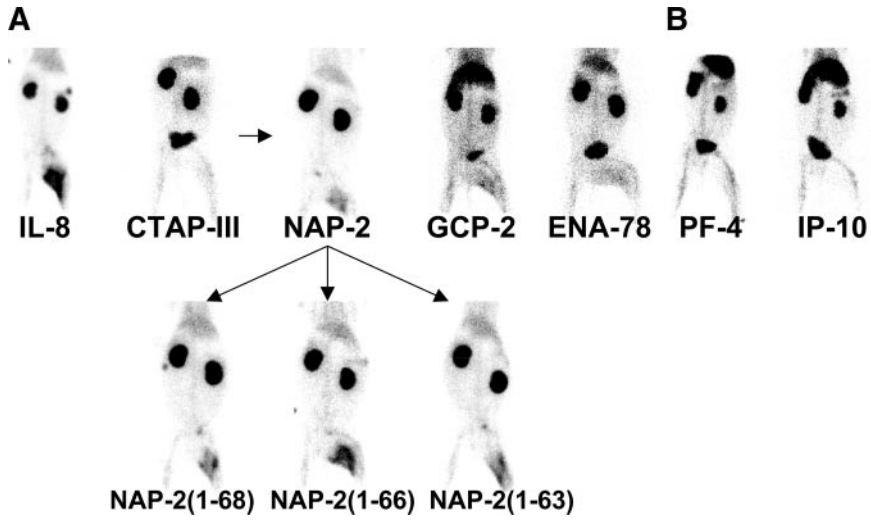

FIGURE 4. Overview of images of rabbits with *E. coli*–induced intramuscular infection obtained 6 h after injection of various ^{99m}Tc-labeled CXC chemokines. (A) ELR$^+$ CXC chemokines: IL-8, CTAP-III, NAP-2 analogs, GCP-2, and ENA-78. (B) ELR$^-$ CXC chemokines: PF-4 and IP-10.

A survey of the ^{99m}Tc-labeled CXC chemokines PF-4, IP-10, CTAP-III, ENA-78, and GCP-2 in infection imaging provided additional evidence for the close relationship between neutrophil-binding affinity and suitability for infection imaging. The presence of an ELR sequence within the CXC chemokine was associated with effective imaging of infection. The ^{99m}Tc-labeled non-ELR CXC chemokines reported in this article, PF-4 and IP-10, lack significant binding to the CXCR1 and the CXCR2 receptor (*10*,*11*) and showed a very low uptake in the abscess. The presence of an ELR sequence may be a prerequisite but does not guarantee effective infection imaging. The radiolabeled ELR$^+$ CXC chemokine CTAP-III showed very low uptake in the abscess as well. CTAP-III is an N-terminally extended precursor of NAP-2. CTAP-III neither binds to or activates neutrophils in sharp contrast to NAP-2. NAP-2 has 1 amino acid residue preceding the ELR sequence and CTAP-III has 16 residues preceding the ELR sequence. It is suggested that the fraying N-terminal end of CTAP-III is interfering with the binding (*23*). In this way, the ELR sequence is masked and functionally not present. The radiolabeled ELR$^+$ CXC chemokines ENA-78 and GCP-2 showed only a modest uptake in the abscess. ENA-78 has high affinity toward the CXCR2 receptor only, but this affinity was found to be lower than that of GCP-2 and considerably lower than that of IL-8. GCP-2 is reported to be efficient in binding the CXCR1 receptor as well (*9*). In the present study, ^{99m}Tc-labeled GCP-2 more clearly delineated infectious foci than ENA-78.

In accordance with these findings are the findings of a comparative study in imaging infection using ^{99m}Tc-labeled C5a and C5a des Arg^{74} (C5adR) (*24*). The complement anaphylatoxin C5a (74 amino acids) differs from its natural metabolite C5adR in just 1 additional C-terminal amino acid residue for C5a. Both act on a common receptor on different cell types, including neutrophils and monocytes. The receptor-binding affinity of C5a exceeds that of C5adR by 1–2 orders of magnitude. For infection imaging, ^{99m}Tc-labeled C5a showed much better characteristics than C5adR: Uptake in the abscess was 5-fold higher for C5a than for C5adR (*24*).

The importance of the C-terminal domain in the function of CXC chemokines was illustrated in this study by radiolabeled NAP-2 and 3 C-terminally truncated isoforms. Differences in biologic (and scintigraphic) behavior are attributed to the physicochemical properties of the deleted residues (*16*). Full-size NAP-2 bears 3 acidic amino acids in the C-terminal end: D_{66}, E_{67}, and D_{70}. The loss of particularly the acidic residues D_{70} and E_{67} caused subsequent increases in biologic activity and binding to neutrophils, and the loss of a third acidic residue in NAP-2 resulted in NAP-2(1–63), the most active NAP-2 isoform. Further deletion of the C-terminal L_{63} was associated with a 3-fold reduction of the capacity of NAP-2(1–63) to bind to and activate neutrophils (*16*). Apparently, L_{63} is a functionally important residue within the structure of NAP-2. The present study showed a discrepancy with these reported findings: Here, the most suitable NAP-2 derivative for infection imaging was radiolabeled NAP-2(1–66), not NAP-2(1–63). This difference might be ascribed to the diverse effects of chemical modification on receptor binding. The chemokines were labeled with ^{99m}Tc using an S-HYNIC derivative as bifunctional agent. S-HYNIC is reacted with primary amino groups—that is, the α-amino group of the N-terminal amino acid residue or the ϵ-amino group of lysine residues within the protein. The conjugation of S-HYNIC might interfere with receptor binding. It is tempting to speculate that the fraying C-terminal end of NAP-2(1–66) might prevent effective reaction of S-HYNIC with the lysines at critical positions 61 and 62 near to L_{63}. This might explain the preferential qualities for infection imaging of ^{99m}Tc-labeled NAP-2(1–66) as compared with NAP-2(1–63).

The importance of the N-terminal domain in the function of the CXC chemokines is exemplified in the pair of closely related proteins CTAP-III and NAP-2 in our study and also in a comparison between 2 naturally existent isoforms of IL-8 (*2*). The most abundant form of naturally occurring IL-8 is 72 amino acids long. This form has 3 residues in front of the ELR sequence. A 77-amino-acid variant of IL-8 is produced by endothelial cells and is extended at the N-terminus by 5 amino acids. The longer protein is some 10-fold less potent than the shorter protein in attracting and activating neutrophils. The differences might, again, be attributed to the negative interference of the longer fraying N-terminal end of IL-8(77) in the binding of the protein to CXC receptors. IL-8(72) has a high affinity for both the CXCR1 and the CXCR2 receptor, and its potency as a neutrophil chemoattractant has been estimated to be 3-fold higher than that of NAP-2 (*25*). The potential of radiolabeled IL-8(72) for imaging infection has been extensively explored by us (*18*–*20*) and, not surprisingly, is superior to that of other CXC chemokines, including the NAP-2 analogs.

CONCLUSION

This study showed a clear relationship between affinity to receptors on neutrophils and suitability for infection imaging. Of the NAP-2 variants, NAP-2(1–66) combined highest affinity to CXCR2 with best characteristics for imaging. IL-8, having a clearly higher affinity for the CXCR1 and CXCR2 receptor than for NAP-2(1–66), showed a superior imaging quality. The other CXC chemokines tested appeared to be less suitable for infection imaging.

REFERENCES

1. Rennen HJ, Boerman OC, Oyen WJ, Corstens FH. Imaging infection/inflammation in the new millennium. *Eur J Nucl Med.* 2001;28:241–252.
2. Rollins BJ. Chemokines. *Blood.* 1997;90:909–928.
3. Abrams MJ, Juweid M, tenKate CI, et al. Technetium-99m-human polyclonal IgG radiolabeled via the hydrazino nicotinamide derivative for imaging focal sites of infection in rats. *J Nucl Med.* 1990;31:2022–2028.
4. Zlotnik A, Yoshie O. Chemokines: a new classification system and their role in immunity. *Immunity.* 2000;12:121–127.

5. Van Damme J. Interleukin-8 and related chemotactic cytokines. In: Thomson AW, ed. *The Cytokine Handbook*. London, U.K.: Academic Press; 1994:185.
6. Feniger-Barish R, Belkin D, Zaslaver A, et al. GCP-2-induced internalization of IL-8 receptors: hierarchical relationships between GCP-2 and other ELR(+)-CXC chemokines and mechanisms regulating CXCR2 internalization and recycling. *Blood.* 2000;95:1551–1559.
7. Lee J, Horuk R, Rice GC, Bennett GL, Camerato T, Wood WI. Characterization of two high affinity human interleukin-8 receptors. *J Biol Chem.* 1992;267: 16283–16287.
8. Ahuja SK, Murphy PM. The CXC chemokines growth-regulated oncogene (GRO) alpha, GRObeta, GROgamma, neutrophil-activating peptide-2, and epithelial cell-derived neutrophil-activating peptide-78 are potent agonists for the type B, but not the type A, human interleukin-8 receptor. *J Biol Chem.* 1996; 271:20545–20550.
9. Wuyts A, Proost P, Lenaerts JP, Ben Baruch A, Van Damme J, Wang JM. Differential usage of the CXC chemokine receptors 1 and 2 by interleukin-8, granulocyte chemotactic protein-2 and epithelial-cell-derived neutrophil attractant-78. *Eur J Biochem.* 1998;255:67–73.
10. Clark-Lewis I, Dewald B, Geiser T, Moser B, Baggiolini M. Platelet factor 4 binds to interleukin 8 receptors and activates neutrophils when its N terminus is modified with Glu-Leu-Arg. *Proc Natl Acad Sci USA.* 1993;90:3574–3577.
11. Dewald B, Moser B, Barella L, Schumacher C, Baggiolini M, Clark-Lewis I. IP-10, a gamma-interferon-inducible protein related to interleukin-8, lacks neutrophil activating properties. *Immunol Lett.* 1992;32:81–84.
12. Brandt E, Petersen F, Ludwig A, Ehlert JE, Bock L, Flad HD. The beta-thromboglobulins and platelet factor 4: blood platelet-derived CXC chemokines with divergent roles in early neutrophil regulation. *J Leukoc Biol.* 2000;67:471–478.
13. Walz A, Baggiolini M. Generation of the neutrophil-activating peptide NAP-2 from platelet basic protein or connective tissue-activating peptide III through monocyte proteases. *J Exp Med.* 1990;171:449–454.
14. Brandt E, Van Damme J, Flad HD. Neutrophils can generate their activator neutrophil-activating peptide 2 by proteolytic cleavage of platelet-derived connective tissue-activating peptide III. *Cytokine.* 1991;3:311–321.
15. Ehlert JE, Petersen F, Kubbutat MH, Gerdes J, Flad HD, Brandt E. Limited and defined truncation at the C terminus enhances receptor binding and degranulation activity of the neutrophil-activating peptide 2 (NAP-2): comparison of native and recombinant NAP-2 variants. *J Biol Chem.* 1995;270:6338–6344.
16. Ehlert JE, Gerdes J, Flad HD, Brandt E. Novel C-terminally truncated isoforms of the CXC chemokine beta-thromboglobulin and their impact on neutrophil functions. *J Immunol.* 1998;161:4975–4982.
17. Krijgsveld J, Zaat SA, Meeldijk J, et al. Thrombocidins, microbicidal proteins from human blood platelets, are C- terminal deletion products of CXC chemokines. *J Biol Chem.* 2000;275:20374–20381.
18. Rennen HJ, Boerman OC, Oyen WJ, van der Meer JW, Corstens FH. Specific and rapid scintigraphic detection of infection with ^{99m}Tc-labeled interleukin-8. *J Nucl Med.* 2001;42:117–123.
19. Rennen HJ, van Eerd JE, Oyen WJ, Corstens FH, Edwards DS, Boerman OC. Effects of coligand variation on the in vivo characteristics of Tc-99m-labeled interleukin-8 in detection of infection. *Bioconjug Chem.* 2002;13:370–377.
20. Gratz S, Rennen HJ, Boerman OC, Oyen WJ, Corstens FH. Rapid imaging of experimental colitis with ^{99m}Tc-interleukin-8 in rabbits. *J Nucl Med.* 2001;42: 917–923.
21. Schwartz DA, Abrams MJ, Giadomenico CM, Zubieta JA, inventors; Johnson Matthey, Inc., assignee. Certain pyridyl hydrazines and hydrazides useful for protein labeling. US patent 5 206 370. May 26, 1992.
22. Loetscher P, Seitz M, Clark-Lewis I, Baggiolini M, Moser B. Both interleukin-8 receptors independently mediate chemotaxis: Jurkat cells transfected with IL-8R1 or IL-8R2 migrate in response to IL-8, GRO alpha and NAP-2. *FEBS Lett.* 1994;341:187–192.
23. Malkowski MG, Lazar JB, Johnson PH, Edwards BF. The amino-terminal residues in the crystal structure of connective tissue activating peptide-III (des10) block the ELR chemotactic sequence. *J Mol Biol.* 1997;266:367–380.
24. Rennen HJ, Oyen WJ, Cain SA, Monk PN, Corstens FH, Boerman OC. Tc-99m-labeled C5a and C5a des Arg^{74} for infection imaging. *Nucl Med Biol.* 2003;30: 267–272.
25. Leonard EJ, Yoshimura T, Rot A, et al. Chemotactic activity and receptor binding of neutrophil attractant/activation protein-1 (NAP-1) and structurally related host defense cytokines: interaction of NAP-2 with the NAP-1 receptor. *J Leukoc Biol.* 1991;49:258–265.